

Topological wormholes: Nonlocal defects on the toric code

Anirudh Krishna  and David Poulin*Département de physique & Institut Quantique, Université de Sherbrooke, Sherbrooke, Québec, Canada J1K 2R1*

(Received 1 October 2019; accepted 3 April 2020; published 1 May 2020)

Locality plays a fundamental role in quantum computation but also severely restricts our ability to store and process quantum information. We argue that this restriction may be unwarranted and re-examine quantum error correcting codes. We proceed to introduce new defects on the surface code called wormholes. These novel defects entangle two spatially separated sectors of the lattice. When anyonic excitations enter the mouth of a wormhole, they emerge through the other mouth. Wormholes thus serve to connect two spatially separated sectors of a flat two-dimensional lattice. We show that these defects are capable of encoding logical qubits and can be used to perform all gates in the Clifford group.

DOI: [10.1103/PhysRevResearch.2.023116](https://doi.org/10.1103/PhysRevResearch.2.023116)

I. INTRODUCTION

Locality plays a central role in condensed matter and quantum information science. This is exemplified by Kitaev's toric code [1], its variants [2], and the color code [3]. These physical models are defined by Hamiltonians composed entirely of local terms of low weight and yet display topological order—the ground states of the system cannot be discerned using local measurements. From the perspective of quantum computation, this means that the code space is robust to local errors as perturbations must collude over a large distance to induce a logical error. Furthermore, the locality of the Hamiltonian is a boon for experimental realizations of quantum error correction and considerably simplifies the syndrome extraction circuits. For this and many other reasons, such models are a promising blueprint for scalable quantum computers [4–6].

Locality, however, poses severe restrictions on storing and processing encoded quantum information [7–9]. Architectures based on nitrogen vacancy (NV) centers and ion traps have softer constraints on coupling qubits that are not adjacent [10]. With the advent of deterministic methods to share entanglement nonlocally on superconducting qubit architectures [11–13], the strict restriction of locality in the design of quantum error correcting codes may be unwarranted. Furthermore, modeling qubits as pointlike objects may not apply to physical implementations which use extended objects such as resonators to store quantum information [14]. In such an architecture, the geometry of qubit couplings may not be suitably represented by a two-dimensional grid. For these reasons, we have chosen to bend the rules of locality and re-examine quantum error correcting codes. The results presented here are independent from the no-go results of Refs. [7] and [8]

which places restrictions on two-dimensional quantum error correcting codes.

In this article, we demonstrate how introducing a small amount of nonlocality gives rise to novel defects on the toric code which we call *wormholes*. These defects possess two mouths that connect two spatially separated sectors of the lattice that we refer to as the mouths of the wormhole. The name is motivated by considering the movement of lattice excitations called anyons. If an anyon were to enter the mouth of a wormhole, then it emerges via the other. In turn, this means that two anyons can be spatially separated by an arbitrary distance and still share entanglement via the wormhole. Furthermore, we shall show that we can use wormholes to encode logical information. We then demonstrate how we can perform all Clifford operations on the logical information. This can be seen as a unification of previous defect-based encoding schemes combining puncture and twist defects [5,15–19].

If we eschew locality entirely, then we can obtain quantum low-density parity-check (LDPC) codes that are capable of encoding a number of qubits that grows with the block size [20–22]. In a companion paper [23], we outline how to generalize the techniques presented here to perform gates on a certain class of LDPC codes called hypergraph product codes [22,24]. Although engineering such connections may be infeasible with current technology, hypergraph product codes have the potential to reduce the overhead associated with constructing quantum circuits in the long term [25,26]. This is the first technique that provides a framework to fault tolerantly perform gates on this family of error correcting codes. This work can also be seen as a proposal for codes in the spectrum between entirely local codes on the one end and quantum LDPC codes on the other.

Last, our construction could contribute to the discussion on the connection between entanglement and the geometry of spacetime [27]. We first note that the geometry that an anyon experiences is dictated by the entanglement in the underlying spin substrate. This is reminiscent of the ER = EPR conjecture in quantum gravity [28]. Second, if we define the entropy of a wormhole as the entanglement entropy between two mouths, then we find that it scales with the size of the boundary of the

mouths rather than the size of the mouths. This mirrors the Bekenstein entropy [29] which also scales proportionally to the area of a black hole.

II. BACKGROUND AND NOTATION

The toric code [2] is a quantum error correcting code defined on a square lattice with periodic boundary conditions. Qubits are placed on the edges of the lattice and the vertices and plaquettes of the lattice serve to define a local Hamiltonian \mathcal{H} . For ease of representation, we introduce some notation.

$$\begin{array}{c} \text{---} \square \text{---} \\ | \\ \text{---} \square \text{---} \end{array} := \begin{array}{c} \bigcirc \\ | \\ \bigcirc \\ | \\ \bigcirc \end{array} \quad \square := \begin{array}{c} \bullet \\ \bullet \\ \bullet \\ \bullet \end{array}$$

Circles on edges represent single-qubit operators on the corresponding qubits—empty circles represent single-qubit Pauli X operators and filled circles represent single-qubit Pauli Z operators. We will later see multiple circles arranged in some pattern and this corresponds to products of the respective Pauli operators. Likewise, each local term or *stabilizer* is a product of Pauli operators and is denoted using a square node—empty square nodes on vertices represent X stabilizers, and dark square nodes on plaquettes represent Z stabilizers. The Hamiltonian is the sum of local terms,

$$\mathcal{H} = - \sum_{+} \begin{array}{c} \text{---} \square \text{---} \\ | \\ \text{---} \square \text{---} \end{array} - \sum_{\square} \square.$$

The first sum is over vertices of the lattice and the second sum is over faces of the lattice. The code space is the ground space of \mathcal{H} .

III. TORIC CODE DEFECTS

The Clifford group is the set of unitary gates which is generated by the Hadamard, phase, and CNOT gates. These gates occupy a special role in the theory of fault tolerance. We begin by describing defects on the toric code that are capable of encoding qubits in a manner that facilitates Clifford gates.

Punctures are defects on the surface code that appear in two varieties, smooth and rough, as shown in Fig. 1. A smooth

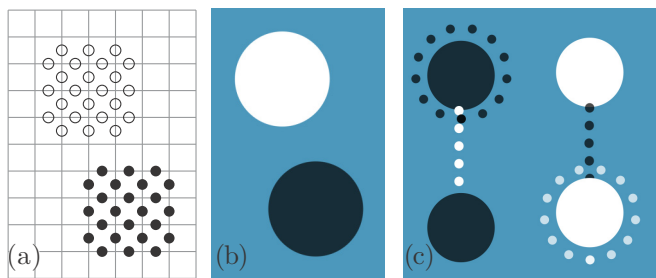


FIG. 1. Smooth and rough punctures on a lattice. (a) Measurements that serve to create the smooth and rough punctures are denoted using empty and filled circles, respectively. (b) Corresponding lattice-free representation with smooth puncture in black and rough puncture in white. (c) Encoding a logical qubit in a pair of smooth or rough punctures.

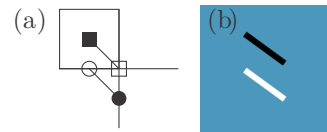


FIG. 2. (a) Two-qubit measurement indicated by two circle nodes and line connecting them. Hybrid stabilizer indicated by square nodes and line connecting them. (b) Lattice-free representation of two-qubit measurement, indicated by a white line, and product of stabilizers, indicated by a black line.

puncture is created by measuring X on the support of a set of X stabilizers, whereas a rough puncture is created by measuring Z on the support of a set of Z stabilizers. A pair of smooth or rough punctures can be used to encode a logical qubit as shown in Fig. 1(c). The logical Z (X) assigned to a pair of smooth (rough) punctures is a loop of Z 's (X 's) encircling a puncture; the conjugate logical X (Z) operator is a chain of X 's (Z 's) between two smooth (rough) punctures.

Braiding punctures results in a logical CNOT with the smooth puncture serving as control and the rough puncture serving as target [5,30]. However, braiding is limited; as such, it maps X operators to X operators and Z operators to Z operators. We need to break this restriction to perform a broader class of gates.

Twists are yet another defect on the toric code that address this issue [15]. These objects are created by measuring two-qubit operators composed of one X and one Z on adjacent qubits. The measurement is depicted in Fig. 2(a) by the two circle nodes and the line connecting them. The individual plaquette and vertex stabilizers incident to these qubits anticommute with this measurement. This pair of stabilizers is replaced by its product to resolve this frustration. It is depicted by the line connecting the two square nodes in Fig. 2(a). As shown in Fig. 3, we can perform two-qubit measurements along a line referred to as a defect line; the hybrid stabilizers at either end of this line are called twists. X and Z stabilizer generators across the defect line pair up to form hybrid stabilizers of weight 6. These objects can be used to supplement the set of possible operations on punctures—a smooth puncture that crosses the defect line is transformed into a rough puncture and vice versa. Furthermore, two pairs of twists can be used to encode a logical qubit in their own

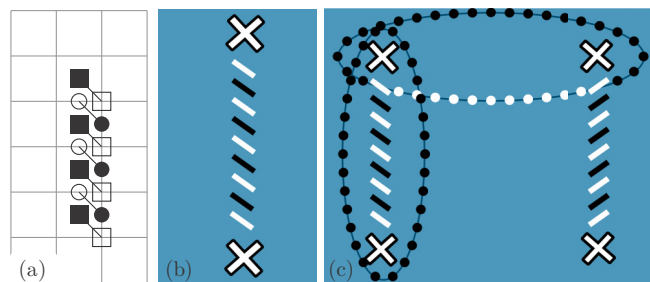
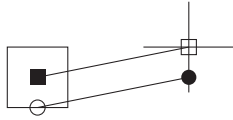


FIG. 3. A twist on a lattice. (a) Measure the pairs of qubits using the two-qubit operator $X \otimes Z$; X on the vertical edges and Z on the horizontal edges. (b) Lattice-free representation of the twist. The twists are marked as white crosses. (c) Encoding a logical qubit in two pairs of twists.

right as shown in Fig. 3(c). The logical Z is the loop of Z 's encircling a pair of twists and the shared defect line. The logical X is a loop that runs between the pair that contains both X and Z operators. We can perform single-qubit Clifford gates on encoded qubits by exchanging twists [15–17,31,32].

IV. WORMHOLES

We introduce a new type of defect called a *wormhole* that can be seen as a marriage of puncture and twist defects. Consider the two-qubit measurement that was used to create a twist but with spatially separated X (white circle) and Z (dark circle) operators as shown.



These are measured on the support of a plaquette and vertex stabilizer respectively. To resolve the anticommutation, we replace these objects by the hybrid stabilizer indicated by the line joining the plaquette and vertex stabilizer generators. We highlight that the support of this object lies in spatially separated parts of the lattice. We remark that in Appendix A 1, we also demonstrate how to move a wormhole using only local measurements. Thus a wormhole can be prepared using short-range connections and then moved to the right location.

All hybrid stabilizers are a product of one plaquette and one vertex generator and thus this code remains LDPC. We can go further by noting that there is no reason to restrict ourselves to measurements along a line. We can measure two-qubit operators along boundaries of punctures as shown in Fig. 4. This creates two entangled punctures that are spatially separated that we refer to as the mouths of the wormhole. These new hybrid stabilizers have weight 6; this is the product of two stabilizers on the boundary, minus their support inside

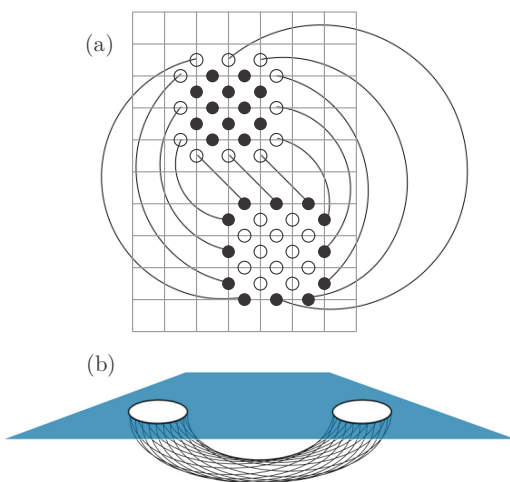


FIG. 4. Creating a wormhole. (a) Measuring two-qubit Pauli operators along the boundary of a puncture. (b) Side view of lattice free representation of the wormhole. The two white circles represent the mouths of the wormhole. The wire mesh underneath the lattice represents the entanglement between these two patches. The mesh is merely a visual aid and does not represent an extension of the lattice.

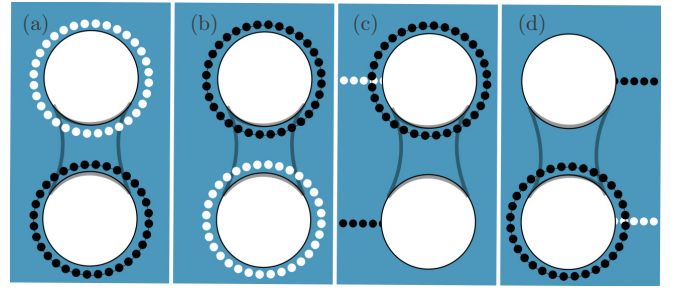


FIG. 5. Stabilizer and logical generators of the wormhole. [(a) and (b)] The stabilizer generators of the wormhole. [(c) and (d)] The logical operators of each logical qubit. The logical Z is a loop of Z operators encircling the mouth of a wormhole. The logical X is composed of two strings that run between the two mouths of the wormholes, one string of Z operators and another string of X operators.

the puncture. As shown in Appendix A 2, this weight can be reduced by spreading the weight among some of the local checks adjacent to these stabilizers.

The mouths of a wormhole are topologically indistinguishable. For this reason, we drop the color of the mouths and without loss of generality, depict both mouths in white. On entering one mouth, an anyon emerges via the other mouth with the opposite charge label. Other types of wormholes are possible that preserve the topological charge of the excitations. In general, wormhole types correspond to topological domain walls. In Ref. [33], Barkeshli and Freedman enumerate the different boundaries that can be used to transform one type of charge to another. In contrast, the focus of our work is to understand how to actually construct wormholes and how to use them for performing gates on LDPC codes.

When a wormhole is created from the vacuum, it is stabilized by a pair of nonlocal operators shown in Figs. 5(a) and 5(b). At first glance, it appears that the weight of these stabilizers scales with the size of the puncture. However, these operators are merely products of the hybrid stabilizers on the boundary. We can use a wormhole to encode two logical qubits as shown in Figs. 5(c) and 5(d) that we label 1 and 2. We represent the logical Z operators as a loop of physical Z operators that encircle one mouth. The conjugate logical operators are pairs of strings, one of X type and another of Z type that run to the mouths. We assume that the strings terminate at a “sink” wormhole elsewhere on the lattice.

V. CLIFFORD GATES

We now turn our attention to performing Clifford gates on a qubit encoded in a wormhole. To this end, we use an ancilla qubit initialized in a wormhole to perform single-qubit Clifford gates.

Suppose we have two qubits, labeled 1 and a , denoting the qubit of interest and the ancilla, respectively. The following lemma summarizes what exactly is needed in order to perform single-qubit Clifford gates on qubit 1.

Lemma 1. Let A and B be distinct, nontrivial single-qubit Pauli operators. Let P and Q be two Pauli operators, not necessarily distinct. The two-qubit measurements $A_1 P_a$ and $B_1 Q_a$, together with all single-qubit Pauli measurements on

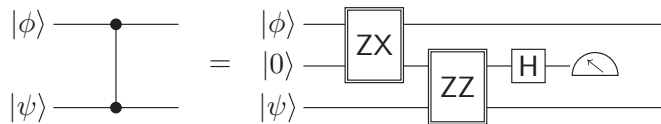


FIG. 6. A measurement-based circuit to perform controlled-Z. We introduce an ancilla prepared in the $|0\rangle$ state. The double-boxes indicate a nondestructive projective measurement. The labels PQ on these measurements indicate that the projection is performed along the $+1$ and -1 eigenstates of the two-qubit Pauli operator PQ. Finally, we perform a Hadamard and destructively measure the ancilla qubit in the computational basis.

qubit a are sufficient to generate the single-qubit Clifford group on qubit 1.

Proof. A logical Clifford operation proceeds in three steps. Without loss of generality, let $P = Q = A$ and consider the measurement of $A_1 P_a$.

- (1) Initialize qubit a by preparing it in the B basis.
- (2) Next, perform a joint measurement $A_1 P_a (= A_1 A_a)$ of qubits 1 and a .
- (3) Finally, measure qubit a in the basis $C (\neq A \neq B \neq I)$.

The following flowchart tracks the transformation of the generators of the associated stabilizer and normalizer groups, S and \mathcal{N} .

$$S = \{B_a\} \rightarrow \{A_1 A_a\} \rightarrow \{C_a\}$$

$$\mathcal{N} = \{B_1, C_1\} \rightarrow \{B_1 B_a, C_1 B_a\} \rightarrow \{C_1 C_a, B_1 C_a\}.$$

We have used the fact that Pauli operators are cyclic, i.e., the product of any two distinct operators yields the third (up to a phase). Up to stabilizer, the result of this transformation is to map B to C and vice versa. The result follows. ■

In addition to single-qubit Clifford gates, we need one entangling gate to generate the Clifford group. This can be performed using just X and Z measurements and an ancilla prepared in the $|0\rangle$ state as shown in Fig. 6.

We now need to demonstrate how to perform such a set of operations fault tolerantly. To this end, we shall use a qubit encoded in a pair of smooth or rough punctures. This qubit, referred to as the needle, can be used to *stitch* logical operators of interest as we shall demonstrate. It will therefore not require any more long-range connectivity beyond what is required to initialize the wormholes

Braiding the needle around one mouth of a wormhole results in the controlled-Z operation between the needle and an encoded qubit. The evolution of the logical X operator of the puncture is shown in Fig. 7.

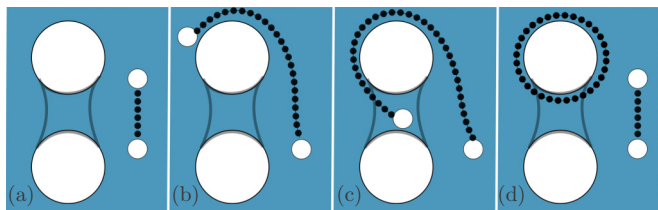


FIG. 7. Braiding the needle around the wormhole results in a controlled-Z operation between the needle and encoded qubit.

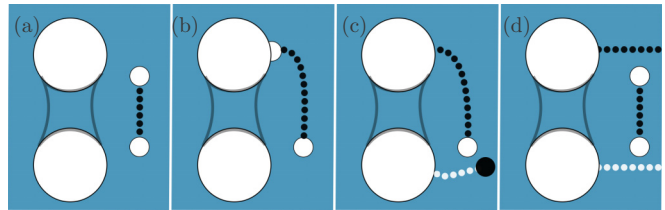


FIG. 8. Passing the puncture through the mouth of the wormhole results in the controlled-X between the needle and encoded qubit. Between panels (c) and (d), the puncture goes through the sink wormhole so as to return to the appropriate type.

Since the wormhole is traversable, a puncture can enter one mouth of the wormhole and emerge via the other. We call this operation *stitching*. Stitching results in the controlled- X operation between the needle and the encoded qubit. The evolution of the logical X of the puncture is shown in Fig. 8.

We define certain properties of the logical operators. First we notice that the needle operators X and Z are efficiently preparable and can be measured fault tolerantly. If we need to measure the stringlike operator that runs between punctures for instance, then we could make the punctures larger and bring them closer together. Alternatively to measure the loop-type operator, we can move the punctures apart, make them small and measure the boundary. The logical X and Z operators will thus be referred to as *needle-measurable* operators. On the other hand, the logical Y operator associated to a puncture is not needle-measurable as this would necessitate shrinking the boundary as well as bringing the punctures close together. In turn, the measurement would no longer be fault tolerant.

An operator Q is *traceable* if there exists a way to map a needle-measurable operator P to PQ . The logical Z operator of a puncture was already traceable. We highlight that by converting a puncture to a wormhole, the logical X operator is now also traceable.

The final ingredient required to perform logical single-qubit Clifford gates as stipulated by Lemma 1 is a Y measurement. Unfortunately, logical Y operators of wormholes are not traceable as the Y operator crosses itself. To be precise, let Y_w denote the logical Y of the wormhole and Y_n be the logical Y of the needle. In following the path of a logical Y_w associated to a wormhole, we find that it is the logical Y_n operator of the needle that is mapped to $Y_n Y_w$. Since the

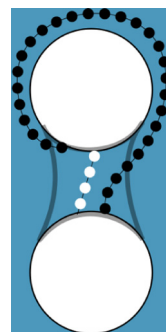


FIG. 9. The product $Y_a Y_b$ does not cross itself and is therefore traceable.

logical Y_n of the needle is not needle-measurable, the logical Y of the wormhole is not traceable.

This is remedied with a resource state as follows. We let a wormhole that can encode 2 qubits serve as the ancilla.

Lemma 2. Let the ancilla be composed of two qubits labeled a and b such that one of its stabilizer generators is $I_a Y_b$. It is possible to apply the measurement $Y_a I_b$ on qubit a fault tolerantly without affecting the state of the generator $I_a Y_b$.

Proof. Let a and b refer to the qubits encoded in a wormhole. However, the product $Y_a Y_b$ is traceable as shown in Fig. 9. This is because the operator does not intersect itself. This can be used to measure $Y_a I_b$ by initializing the wormhole in a state such that $I_a Y_b$ is a stabilizer generator. We can then measure $Y_a Y_b$, which up to action of an element of the stabilizer, is equivalent to $Y_a I_b$. The generator $I_a Y_b$ commutes with the measurement and is therefore unaffected. It can therefore be used for the next gate as well and in this sense, the gate is catalytic. ■

The intuition behind this claim is that the operator $Y_a Y_b$ does not cross itself and hence is traceable. Assuming such a resource state is provided ahead of time, we can perform catalytic Clifford gates. Together with stitching and braiding, this completes the requirements to generate the Clifford group as per Lemma 1.

VI. DISCUSSION AND CONCLUSION

We have introduced a new defect on the toric code called a wormhole using entangled measurements along the bound-

aries of punctures. This leads to interesting physics when we consider the movement of anyons on the surface of the lattice. Wormholes are capable of encoding a logical qubit and facilitate all gates in the Clifford group. Importantly, wormholes provide a way to perform fault-tolerant gates on a class of quantum LDPC codes called hypergraph product codes.

ACKNOWLEDGMENTS

We thank Colin Trout for detailed comments on an earlier draft of this work, Baptiste Royer for discussions on deterministic entanglement sharing in superconducting qubit architectures and Ben Criger for discussions on code deformation. A.K. acknowledges support from the Fonds de recherche du Québec–Nature et technologies (FRQNT) via the B2X scholarship for doctoral candidates. David Poulin is a CIFAR Fellow with the Quantum Information Science program.

APPENDIX

1. Moving defects

In this section, we demonstrate how to move an elementary defect using only local two-qubit measurements. This elementary defect is the product of X and Z stabilizers that are spatially separated. We demonstrate how to move this defect on only one side as shown in Fig. 10. In particular, we shall move the Z support of the stabilizer using only local measurements. In the diagram, stabilizer operators shall be

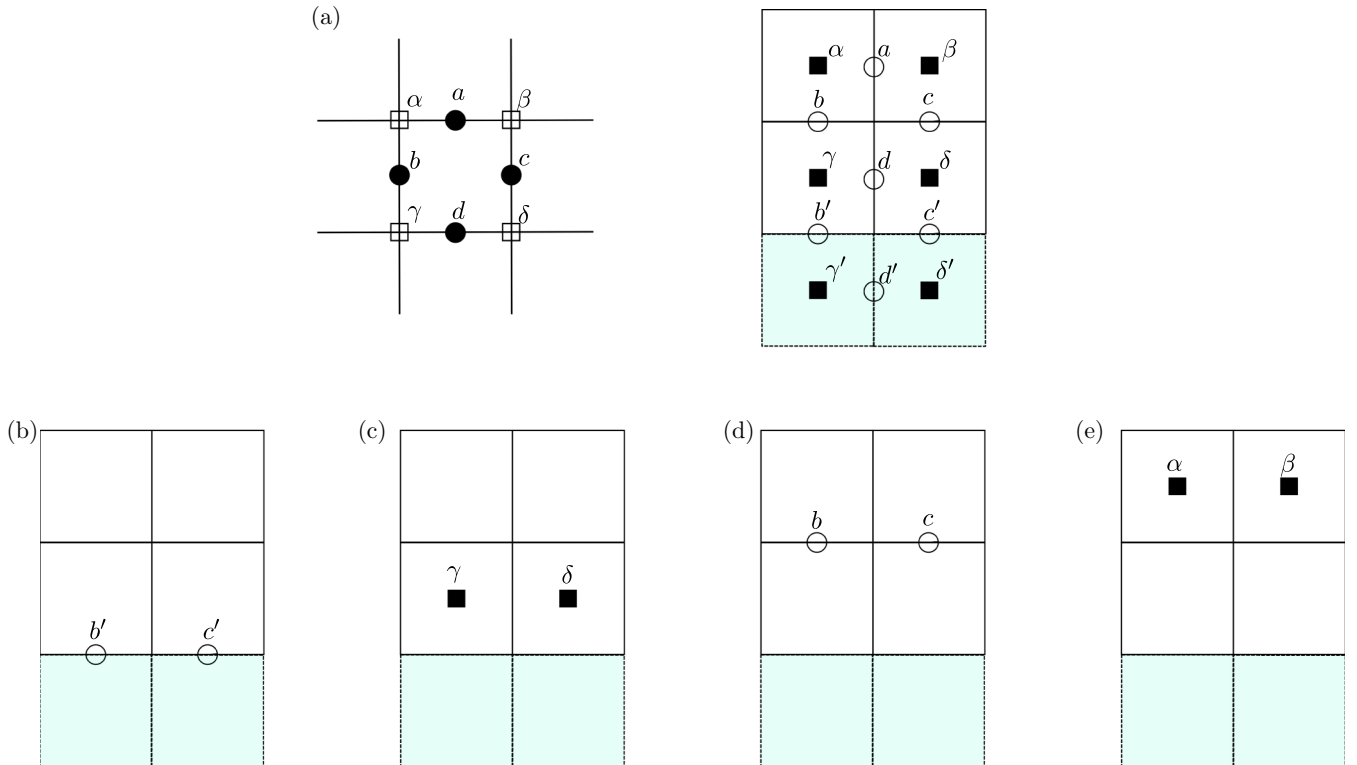


FIG. 10. Translating a wormhole using local measurements. Panel (a) shows the support of the hybrid stabilizers. These stabilizers could potentially be in separate regions of the surface code lattice. This panel also establishes the names of the different nodes that we have used in the main body of the text. Panels (b)–(e) show step-by-step the measurements that need to be performed in order to translate the Z -type support of the defect.

labeled using greek letters and qubits shall be labeled using latin lowercase letters. Furthermore, X_α shall represent X stabilizer α and X_a will denote the single-qubit X operator on the qubit a .

Step 0. Figure 10(a) depicts the initial step. Joint measurements are labeled using the same latin lowercase letters. Therefore, the black node a (on the left) and the white node a (on the right) refer to a joint measurement of $Z_a X_a$ and so on. This induces the hybrid stabilizers; these are also labeled using the same Greek letters. Thus the hybrid stabilizers would be $X_\alpha Z_\alpha$ and so on. The objective will be to move the support of the smooth puncture down by one lattice unit. The new lattice is labeled similarly using primed alphabets.

Step 1. As in Fig. 10(b), measure the operators $X_b X_{c'}$. This measurement anticommutes with

- (1) the hybrid stabilizers $X_\gamma Z_\gamma$ and $X_\delta Z_\delta$; and
- (2) the plaquette operators $Z_{\gamma'}$ and $Z_{\delta'}$.

We replace these stabilizers with the products $X_\gamma Z_\gamma Z_{\gamma'}$ and $X_\delta Z_\delta Z_{\delta'}$. Perform the measurement $Z_d Z_{d'}$.

Step 2. As shown in Fig. 10(c), measure the plaquette operators Z_γ and Z_δ . These measurements anticommute with

- (1) the two-qubit operators $Z_b X_b$ and $Z_c X_{c'}$; and
- (2) the single-qubit operator $X_{b'}$ and $X_{c'}$.

We replace these operators by the products $Z_b X_b X_{b'}$ and $Z_c X_c X_{c'}$. It also anticommutes with $Z_d X_d$ and $X_d X_{d'}$; we replace them with their product $Z_d X_d$. Measuring the plaquette operators Z_γ and Z_δ returns them to the stabilizer. We can now update the hybrid stabilizers by multiplying them by these stabilizers as

$$X_\gamma Z_\gamma Z_{\gamma'} \rightarrow X_\gamma Z_{\gamma'} \quad X_\delta Z_\delta Z_{\delta'} \rightarrow X_\delta Z_{\delta'}.$$

Step 3. As shown in Fig. 10(d), measure the single-qubit operators X_b and $X_{c'}$. These measurements anticommute with

- (1) the plaquette operators Z_γ and Z_δ ; and
- (2) the hybrid operators $X_\alpha Z_\alpha$ and $X_\beta Z_\beta$.

We replace these operators by the products $X_\alpha Z_\alpha Z_\gamma$ and $X_\beta Z_\beta Z_\delta$. Perform the measurement $X_a X_d$. We can also perform the following reductions:

$$Z_b X_b X_{b'} \rightarrow Z_b X_{b'} \quad Z_c X_c X_{c'} \rightarrow Z_c X_{c'}.$$

Step 4. As shown in Fig. 10(e), measure the plaquette operators Z_α and Z_β . These measurements anticommute with

- (1) the single-qubit operators X_b and $X_{c'}$; and
- (2) the two-qubit operators $Z_a X_a$ and $X_a X_d$.

We replace these operators by the product $Z_a X_d$. We can also perform the following reductions

$$X_\alpha Z_\alpha Z_\gamma \rightarrow X_\alpha Z_\gamma \quad X_\beta Z_\beta Z_\delta \rightarrow X_\beta Z_\delta.$$

This completes the translation.

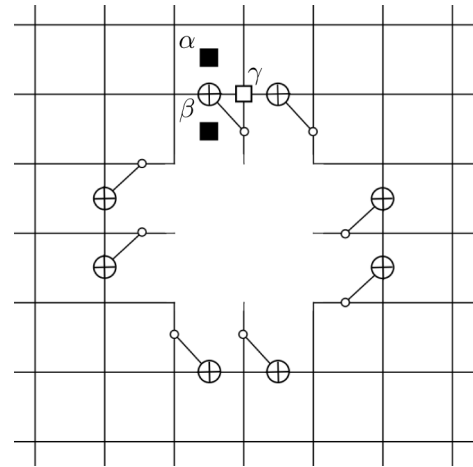
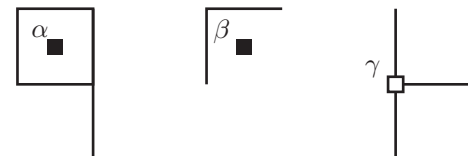


FIG. 11. Using CNOT gates to lower the weight of hybrid stabilizers.

2. Reducing the weight of stabilizers

In this subsection, we indicate how one can reduce the weight of the hybrid stabilizers. The idea is to use local measurements to “trade” the weight of the hybrid stabilizers with that of the neighboring stabilizers. This is illustrated in Fig. 11. The figure shows one mouth of a wormhole, and we perform CNOT gates along the boundary as shown. This changes the weights of the some stabilizers that are adjacent to the mouth. In addition to the hybrid stabilizers, the weight of the adjacent plaquette operators increases, and the weight of the adjacent vertex operators decreases. Consider the stabilizers labeled α , β , and γ .



The Z stabilizer α , previously a regular plaquette operator becomes a five-qubit operator. Its weight has increased by 1. The operator β , which is part of the hybrid stabilizer, becomes a three-qubit operator. Together with its X counterpart, the weight of the hybrid stabilizer is now also 5. Finally, the X stabilizer γ , previously a vertex operator, becomes a three-qubit operator. Its weight has decreased by 1.

This intuition extends to larger punctures as well. In this way, we can use CNOT gates to reduce the weight of hybrid stabilizers from 6 to 5 by using CNOT gates to spread the weight among the neighboring stabilizers.

[1] A. Y. Kitaev, Fault-tolerant quantum computation by anyons, *Ann. Phys.* **303**, 2 (2003).
[2] S. B. Bravyi and A. Y. Kitaev, Quantum codes on a lattice with boundary, [arXiv:quant-ph/9811052](https://arxiv.org/abs/quant-ph/9811052) (1998).
[3] H. Bombin and M. A. Martin-Delgado, Topological Quantum Distillation, *Phys. Rev. Lett.* **97**, 180501 (2006).

[4] R. Raussendorf, J. Harrington, and K. Goyal, A fault-tolerant one-way quantum computer, *Ann. Phys.* **321**, 2242 (2006).
[5] R. Raussendorf and J. Harrington, Fault-Tolerant Quantum Computation with High Threshold in Two Dimensions, *Phys. Rev. Lett.* **98**, 190504 (2007).

- [6] R. Raussendorf, J. Harrington, and K. Goyal, Topological fault-tolerance in cluster state quantum computation, *New J. Phys.* **9**, 199 (2007).
- [7] S. Bravyi, D. Poulin, and B. Terhal, Tradeoffs for Reliable Quantum Information Storage in 2D Systems, *Phys. Rev. Lett.* **104**, 050503 (2010).
- [8] S. Bravyi and R. König, Classification of Topologically Protected Gates for Local Stabilizer Codes, *Phys. Rev. Lett.* **110**, 170503 (2013).
- [9] P. Webster and S. D. Bartlett, Braiding defects in topological stabiliser codes of any dimension cannot be universal, *arXiv:1811.11789* (2018).
- [10] N. H. Nickerson, Y. Li, and S. C. Benjamin, Topological quantum computing with a very noisy network and local error rates approaching one percent, *Nat. Commun.* **4**, 1756 (2013).
- [11] P. Kurpiers, P. Magnard, T. Walter, B. Royer, M. Pechal, J. Heinsoo, Y. Salathé, A. Akin, S. Storz, J.-C. Besse *et al.*, Deterministic quantum state transfer and remote entanglement using microwave photons, *Nature* **558**, 264 (2018).
- [12] C. J. Axline, L. D. Burkhardt, W. Pfaff, M. Zhang, K. Chou, P. Campagne-Ibarcq, P. Reinhold, L. Frunzio, S. M. Girvin, L. Jiang *et al.*, On-demand quantum state transfer and entanglement between remote microwave cavity memories, *Nat. Phys.* **14**, 705 (2018).
- [13] P. Campagne-Ibarcq, E. Zalys-Geller, A. Narla, S. Shankar, P. Reinhold, L. Burkhardt, C. Axline, W. Pfaff, L. Frunzio, R. J. Schoelkopf, and M. H. Devoret, Deterministic Remote Entanglement of Superconducting Circuits Through Microwave Two-Photon Transitions, *Phys. Rev. Lett.* **120**, 200501 (2018).
- [14] H. G. Katzgraber, F. Hamze, and R. S. Andrist, Glassy Chimeras Could be Blind to Quantum Speedup: Designing Better Benchmarks for Quantum Annealing Machines, *Phys. Rev. X* **4**, 021008 (2014).
- [15] H. Bombin, Topological Order with a Twist: Ising Anyons From an Abelian Model, *Phys. Rev. Lett.* **105**, 030403 (2010).
- [16] H. Bombin, Clifford gates by code deformation, *New J. Phys.* **13**, 043005 (2011).
- [17] B. J. Brown, K. Laubscher, M. S. Kesselring, and J. R. Wootton, Poking Holes and Cutting Corners to Achieve Clifford Gates with the Surface Code, *Phys. Rev. X* **7**, 021029 (2017).
- [18] Y.-J. Han, R. Raussendorf, and L.-M. Duan, Scheme for Demonstration of Fractional Statistics of Anyons in an Exactly Solvable Model, *Phys. Rev. Lett.* **98**, 150404 (2007).
- [19] M. H. Zarei, General scheme for preparation of different topological states on cluster states, *Phys. Rev. A* **95**, 062316 (2017).
- [20] M. H. Freedman, D. A. Meyer, and F. Luo, Z2-systolic freedom and quantum codes, in *Mathematics of Quantum Computation* (Chapman & Hall/CRC, London, 2002), pp. 287–320.
- [21] L. Guth and A. Lubotzky, Quantum error correcting codes and 4-dimensional arithmetic hyperbolic manifolds, *J. Math. Phys.* **55**, 082202 (2014).
- [22] J.-P. Tillich and G. Zémor, Quantum LDPC codes with positive rate and minimum distance proportional to the square root of the blocklength, *IEEE Trans. Inf. Theory* **60**, 1193 (2014).
- [23] A. Krishna and D. Poulin, Fault-tolerant gates on hypergraph product codes, *arXiv:1909.07424* (2019).
- [24] A. Leverrier, J.-P. Tillich, and G. Zémor, Quantum expander codes, in *Proceedings of the 2015 IEEE 56th Annual Symposium on Foundations of Computer Science (FOCS'15)* (IEEE, Los Alamitos, CA, 2015), pp. 810–824.
- [25] O. Fawzi, A. Grospellier, and A. Leverrier, Constant overhead quantum fault-tolerance with quantum expander codes, in *Proceedings of the 2018 IEEE 59th Annual Symposium on Foundations of Computer Science (FOCS'18)* (IEEE, Los Alamitos, CA, 2018), pp. 743–754.
- [26] O. Fawzi, A. Grospellier, and A. Leverrier, Efficient decoding of random errors for quantum expander codes, in *Proceedings of the 50th Annual ACM SIGACT Symposium on Theory of Computing* (ACM Press, New York, 2018), pp. 521–534.
- [27] F. Pastawski, B. Yoshida, D. Harlow, and J. Preskill, Holographic quantum error-correcting codes: Toy models for the bulk/boundary correspondence, *J. High Energy Phys.* **06** (2015) 149.
- [28] L. Susskind, Copenhagen vs Everett, teleportation, and ER = EPR, *Fortschr. Phys.* **64**, 551 (2016).
- [29] J. D. Bekenstein, Black holes and entropy, *Phys. Rev. D* **7**, 2333 (1973).
- [30] A. G. Fowler, M. Mariantoni, J. M. Martinis, and A. N. Cleland, Surface codes: Towards practical large-scale quantum computation, *Phys. Rev. A* **86**, 032324 (2012).
- [31] T. J. Yoder and I. H. Kim, The surface code with a twist, *Quantum* **1**, 2 (2017).
- [32] H. Zheng, A. Dua, and L. Jiang, Demonstrating non-abelian statistics of majorana fermions using twist defects, *Phys. Rev. B* **92**, 245139 (2015).
- [33] M. Barkeshli and M. Freedman, Modular transformations through sequences of topological charge projections, *Phys. Rev. B* **94**, 165108 (2016).